Synthesis and Characterization of Core–Shell Star Copolymers for In Vivo PET Imaging Applications

Ken-ichi Fukukawa,[†,||] Raffaella Rossin,[‡,||] Aviv Hagooly,[‡] Eric D. Pressly,[†] Jasmine N. Hunt,[†] Benjamin W. Messmore,[†] Karen L. Wooley,[‡,§] Michael J. Welch,[‡,§] and Craig J. Hawker*[,†]

Materials Research Laboratory, Departments of Chemistry, Biochemistry, and Materials, University of California, Santa Barbara, California 93106 and Departments of Chemistry and Radiology, Washington University, Schools of Arts & Sciences and Medicine, St. Louis, Missouri 63110

Received December 21, 2007; Revised Manuscript Received February 6, 2008

The synthesis of core–shell star copolymers via living free radical polymerization provides a convenient route to three-dimensional nanostructures having a poly(ethylene glycol) outer shell, a hydrophilic inner shell bearing reactive functional groups, and a central hydrophobic core. By starting with well-defined linear diblock copolymers, the thickness of each layer, overall size/molecular weight, and the number of internal reactive functional groups can be controlled accurately, permitting detailed structure/performance information to be obtained. Functionalization of these polymeric nanoparticles with a DOTA-ligand capable of chelating radioactive ^{64}Cu nuclei enabled the biodistribution and in vivo positron emission tomography (PET) imaging of these materials to be studied and correlated directly to the initial structure. Results indicate that nanoparticles with increasing PEG shell thickness show increased blood circulation and low accumulation in excretory organs, suggesting application as in vivo carriers for imaging, targeting, and therapeutic groups.

Introduction

The ability to control the structure and composition of nanomaterials is of great importance in the development of nanomedical tools for the diagnosis and treatment of many diseases,[1,2] as their size, composition, physical properties, and surface chemistry influence the behavior of nanomaterials in vivo.[3] To understand and fine-tune these parameters, appropriate synthetic strategies need to be developed, which will allow for the preparation of multifunctional nanostructures. For example, the short lifetime of systemically administered small molecules in the bloodstream can be lengthened significantly by conjugating hydrophilic polymers, especially poly(ethylene glycol) (PEG).[3–14] Although the mechanism responsible for the prolonged blood circulation time of PEGylated systems is controversial,[15] it is generally agreed that the PEG chains form a protective layer, interfering with opsonin adsorption and complement activation and thereby slowing their recognition by the macrophages of the mononuclear monocyte system (MPS).[3,11,16,17] PEGylation, therefore, is an attractive peripheral modification to tune blood circulation lifetimes, which is of paramount importance in the development of novel biomaterials for medical applications.

A variety of different nanostructures has been examined for in vivo applications. For example, micelles have been investigated for drug delivery applications,[18–24] where the hydrophobic assembly of amphiphilic polymers or surfactants in water can effectively encapsulate hydrophobic drugs. However, their use in vivo raises concern due to the reversible nature of micelle formation, leading to a possible instability of these systems at concentrations below their critical micelle concentration (CMC).[25,26] The CMC of polymeric amphiphiles depends on several factors, including size, composition, relative hydrophobic and hydrophilic block lengths, pH, and temperature.[25,26]

To overcome CMC restrictions, covalent stabilization of micelles through core or shell cross-linking has been explored to enhance the capabilities of micelles as drug delivery agents.[27–34] An alternative to these micelle-derived systems are star copolymers, where linear polymer chains are covalently linked to a central core giving rise to a three-dimensional nanostructure. The particular star copolymers, studied herein, have a similar structure to core-cross-linked micelles in their form, but differ in that all "arms" are covalently conjugated to a microgel core during a controlled polymerization step, allowing for the production of polymeric nanostructures with a large range of functional groups and monomer building blocks. For example, fully hydrophilic, heteroarm, and block copolymer star nanostructures can be prepared directly without any limitations or postassembly modifications that might occur or be required for a self-assembly process. Star-like copolymers have been synthesized by various living free radical polymerization methodologies based on an arm-first approach, such as copper-mediated atom transfer radical polymerization (ATRP),[35–37] nitroxide-mediated radical polymerization (NMP),[38–40] (*N*,*N*-diethyldithiocarbamyl)-methylstyrene-mediated radical polymerization,[41] as well as ionic polymerizations.[42–46] Radical polymerization techniques are preferable to other polymerization techniques because of their high functional group tolerance and the ability to introduce a variety of different functional groups orthogonally, allowing for the polymerizations of several different monomers.[47]

In designing synthetic systems for in vivo applications, one of the most important criteria is blood circulation lifetimes and the fate of the nanostructures in the body. As a result, it is

* To whom correspondence should be addressed. E-mail: hawker@mrl.ucsb.edu. Telephone: (805) 893-7161. Fax: (805)893-8797.
† Materials Research Laboratory, Departments of Chemistry, Biochemistry, and Materials, University of California, Santa Barbara.
‡ Division of Radiological Sciences, Washington University School of Medicine, St. Louis, Missouri.
§ Department of Chemistry, Washington University, St. Louis, Missouri.
|| These authors contributed equally to this work.

10.1021/bm7014152 CCC: $40.75
Published on Web 03/13/2008

important to introduce functional groups that allow for imaging and detection of the nanostructures without any detrimental effect on biodistribution. Consequently, positron emission tomography (PET) was chosen as an imaging technique that is commonly used in clinical practice to detect disease states noninvasively with high sensitivity and specificity. The use of PET to image the distribution of a tracer in vivo relies on the presence of a positron-emitting radionuclide within the molecule. Among the positron emitters, ^{64}Cu (β^+: 0.653 MeV, 17.8%; β^-: 0.578 MeV, 39.0%) is currently under investigation for both PET and radiotherapeutic applications.[48] Furthermore, because of its half-life (12.7 h), ^{64}Cu was recently used to evaluate the in vivo distribution and targeting capabilities of polymeric nanoparticles functionalized with tetraazamacrocyclic chelators.[33,49–51]

Herein, we report the synthesis, via NMP, of a series of well-defined, functionalized PEGylated star-shaped copolymers containing a core–shell morphology with DOTA (1,4,7,10-tetraazacyclododecane-1,4,7,10-tetraacetic acid) functional groups in the inner shell, which are available for ^{64}Cu-labeling while at the same time being screened by an outer PEG shell. Within this body of work, star-like copolymers and the linear arm copolymers used to generate them are evaluated in vivo by means of biodistribution experiments and small animal PET imaging.

Experimental Section

Materials. All chemicals were purchased from Sigma-Aldrich Co. (St. Louis, MO), including monomethoxy poly(ethylene glycol) (M_n 2 kDa), *N*,*N*-dimethylacrylamide (DMA), ethylene glycol diacrylate (EGDA, 90% tech), and divinylbenzene (DVB, 90% tech, isomer mixture) and were used without further purification unless otherwise stated. Monomethoxy poly(ethylene glycol) (M_n 5 kDa) was purchased from Nektar Co. (San Carlos, CA) and was used as received. Anhydrous grade *N*,*N*-dimethylformamide (DMF) was used as a solvent. 1,4,7,10-Tetraazacyclododecane-1,4,7-tris(acetic acid-*t*-butyl ester)-10-acetic acid (DOTA) (**1**) was purchased from Macrocyclics Co. (Dallas, TX). 2,2,5-Trimethyl-4-phenyl-3-azahexane-3-nitroxide (α*H* nitroxide) and methyl-(2,2,5-trimethyl-3-(benzylethoxy)-4-phenyl-3-azahexane-poly(ethylene glycol) (Unimer-*x*kPEG, $x = 2, 5$) were synthesized according to the literature, respectively.[52,53] *N*-Acryloxysuccinimide (NAS) was synthesized according to the literature.[54] ^{64}Cu was prepared in the Washington University Medical School CS-15 Cyclotron by the ^{64}Ni(p,n) ^{64}Cu nuclear reaction with a specific activity of 50–200 mCi/μg at the end of bombardment as previously described.[55] Sets of Centricon tubes (YM-30: MWCO 30 kDa; YM-100: 100 kDa) were purchased from Millipore Co. (Billerica, MA). The aqueous buffers used for ^{64}Cu-labeling were treated with Chelex-100 resin, obtained from Bio-Rad Laboratories Co. (Hercules, CA), before use. Zeba desalt spin columns (0.5 and 2 mL) were purchased from Pierce. Hi-Trap desalting columns were purchased from GE Health Biosciences Co. (Princeton, NJ). Radiochemical-thin layer chromatography (radio-TLC) was performed on instant TLC plates (Pall ITLC-SG plates, VWR International, Batavia, IL) and read by a Bioscan 200 imaging scanner (Washington, DC).

Characterization. ^{1}H NMR (200 MHz) and ^{13}C NMR (500 MHz) measurements were performed on Bruker 200 and 500 MHz spectrometers at room temperature, using the solvent proton signal for reference. Apparent molecular weights (MW) and polydispersity index (PDI) values of polymers were obtained using gel permeation chromatography (GPC), equipped with a differential refractive index (RI) detector (Waters Co., model 2414) and four columns (Waters Co., Styragel HR 0.5, 2, 4, and 5) (Milford, MA). DMF, containing 0.1 wt % LiBr, was used as an eluent (flow rate: 1.0 mL/min) at 30 °C; calibration was conducted with linear polystyrene standards. Absolute MW and PDI were obtained using GPC equipped with a multiangle light scattering (MALS) detector (Wyatt Technology Co., DAWN EOS, He−Ne 633 nm laser), a RI detector (Wyatt Technology Co., Optilab DSP and QELS, Santa Barbara, CA), and four columns (300 mm × 8.00 mm, MZ-Gel SD plus 100 Å, MZ-Gel SD plus 10^3 Å, MZ-Gel SD plus 10^5 Å GPC columns); chloroform was used as the eluent (flow rate: 1.0 mL/min) at 25 °C. ASTRA software (Wyatt Technology Co., Santa Barbara, CA) was used to determine the absolute MWs.

Dynamic Light Scattering. Hydrodynamic diameter (D_h) values of nanoparticles in water were determined by dynamic light scattering (DLS). A Brookhaven Instruments Co. (Holtsville, NY) DLS system, equipped with a model BI-9000AT digital autocorrelator, an Avalanche photodiode detector, and a MG vertically polarized 35 mmV He−Ne 633 nm laser, was used at a fixed 90° scattering angle operated by the 9KDLSW control program. For sample preparation, each copolymer (5 mg) was dissolved in DMSO (0.1 mL), followed by deionized water (2.0 mL), added gradually to make a ca. 0.2 wt % aqueous solution. The solution was filtered through a 0.45 μm PTFE membrane filter prior to measurement. All samples were run in triplicate for 10 min at 25 ± 0.2 °C. The D_h and particle size distributions were determined by fitting the correlation functions with ISDA analysis software package and applying CONTIN (Brookhaven Instruments Co.).

Radiolabeling of the DOTA Nanoparticles with ^{64}Cu. The labeling yields for the ^{64}Cu-labeled copolymers were determined by instant thin layer chromatography (ITLC). Aliquots (1.0 μL) of the labeling mixtures were spotted on ITLC-SG plates (Pall, VWR International Co.) and developed in a 1:1 mixture of methanol and 10% (w/v) ammonium acetate. Radio-TLC analysis was performed on a Bioscan 200 imaging scanner (Bioscan Co.). Radiochemical purity (RCP) of the ^{64}Cu-labeled copolymers was monitored by fast protein liquid chromatography (FPLC). FPLC and radio-FPLC were performed using an ÄKTA FPLC system (GE Healthcare Biosciences Co., Princeton, NJ) equipped with a Beckman 170 radioisotope detector (Beckman Instruments Co., Fullerton, CA). A 100 μL analyte was injected into a Superose 12 gel filtration column (GE Healthcare Biosciences Co., Princeton, NJ) and eluted with 20 mM HEPES and 150 mM $NaCl_{(aq)}$ (pH 7.3) at 0.8 mL/min. The UV wavelength was preset to 280 nm, and the radioactivity was monitored by an in-line radio detector.

General Synthesis of PEG-*b*-P(DMA-*co*-NAS) Diblock Arm Copolymer (a1−a4). A mixture of Unimer-2kPEG (1.70 g, 0.723 mmol), DMA (10.1 g, 102 mmol), NAS (1.72 g, 10.2 mmol), α*H* nitroxide (0.0080 g, 0.036 mmol), and DMF (1.35 g) was degassed by freeze–pump–thaw (3 cycles) and sealed under vacuum in an ampule. The vial was then heated at 120 °C for 25 h. After quenching the reaction at 0 °C in iced water, the ampule was opened. The mixture was dissolved in tetrahydrofuran (THF) and precipitated into cold diethyl ether. The precipitate was then collected and dried in vacuo to obtain a white solid (yield: 10.9 g, 81%, **a2**). M_n ($CHCl_3$): 20.6 kDa, PDI: 1.06. M_n (DMF): 59.0 kDa, PDI: 1.16. ^{1}H NMR ($CDCl_3$, δ, ppm): 1.05–2.00 (m, CH, CH_2), 2.70–3.30 (br m, $CNCH_3$, succinimide CH_2), 3.39 (s, OCH3), 3.50–3.85 (s, OCH_2CH_2O).

General Procedure for Formation of Star-Shaped Copolymers (s(1–4)-(e/d)). A solution of the arm copolymer (**a3**) (0.685 g, 0.0601 mmol), DMA (0.0600 g, 0.605 mmol), EGDA (0.104 g, 0.611 mmol), and α*H* nitroxide (0.0006 g, 0.0027 mmol) in DMF (3.40 g, as ca. 20 wt % solution) was degassed by 3 cycles of freeze–pump–thaw, sealed in an ampule, and heated at 120 °C for 46 h (desired time in the range of 22–50 h for the other star-shaped copolymers). After quenching the reaction in iced water, the mixture was poured into cold diethyl ether. The precipitate was then collected and dried in vacuo. Fractional precipitation was carried out with an acetone/hexanes combination several times until the remaining arm copolymers were removed to yield a white powder (yield: 0.242 g, 29%, **s3-e**). M_n ($CHCl_3$): 201 kDa, PDI: 1.15. M_n (DMF): 192 kDa, PDI: 1.22. ^{1}H NMR ($CDCl_3$, δ, ppm): 1.05–2.00 (m, CH, CH_2), 2.70–3.30 (br m, $CNCH_3$, succinimide CH_2), 3.39 (s, OCH3), 3.50–3.85 (s, OCH_2CH_2O).

1,4,7,10-Tetraazacyclododecane-1,4,7-tris(acetic acid-*t*-butyl ester)-10-acetic acid-*N*-Cbz-hexamethylene amide(2).[56,57] Compound **1** (1.00 g, 1.75 mmol) and *N*-hydroxysuccinimide (NHS, 0.502 g, 4.37 mmol) were dissolved in anhydrous DMF (10 mL). After the solution was cooled to 0 °C, *N*,*N*,*N*′,*N*′-tetramethyl-*O*-(1*H*-benzotriazol-1-yl)uronium hexafluorophosphate (HBTU, 0.761 g, 2.01 mmol) and triethylamine (TEA, 0.265 g, 2.62 mmol) were added to the solution, and the mixture was stirred for 15 min. *N*-Cbz-1,6-hexanediamine hydrochloride (0.526 g, 1.83 mmol) was then added, and the mixture was stirred for 16 h at room temperature. The solution was diluted with CH_2Cl_2 (50 mL) and washed with water (4 × 20 mL). The organic layer was dried over anhydrous $MgSO_4$. The excess solvent was evaporated under vacuum, and the residue was purified by column chromatography (CH_2Cl_2/MeOH = 10/1). Yield: 1.28 g, 91%. ^{1}H NMR ($CDCl_3$, δ, ppm): 1.20–1.60 (m, 35H, *t*Bu, $(CH_2)_4$), 2.70–3.70 (m, 28 H, NC $H_2(CH_2)_5$, NCH_2CH_2N, NCH_2CO), 5.09 (s, 2H, $PhCH_2$), 6.02 (s, 1H, NH), 6.51 (s, 1H, NH), 7.35 (s, 5H, Ph). ^{13}C NMR ($CDCl_3$, δ, ppm): 25.5, 26.3, 27.9, 29.2, 29.8, 38.1, 39.3, 55.6, 55.9, 66.6, 81.8, 128.1, 128.5, 136.7, 156.6, 169.9, 171.0, 172.5. MS (ESI$^+$/TOF, *m*/*z*): 827.5 ([M + Na]$^+$, calcd 827.5).

1,4,7,10-Tetraazacyclododecane-1,4,7-tris(acetic acid-*t*-butyl ester)-10-acetic acid-*N*′-amide-hexamethylene diamine (3). Compound **2** (0.674 g, 1.00 mmol) was dissolved in methanol (15 mL)/THF (5 mL) and then Pd/C (10 wt %, 0.110 g) was added into the solution. The solution was stirred vigorously under hydrogen atmosphere at room temperature for 30 h. The Pd/C catalyst was removed by filtration on Celite, and the solvent was evaporated under vacuum to give **3** as a white solid. Yield: 0.504 g (90%). ^{1}H NMR ($CDCl_3$, δ, ppm): 1.20–1.60 (m, 35H, *t*Bu, $(CH_2)_4$), 2.46 (m, 2H, $(CH_2)_5C$ H_2NH_2), 2.70–3.70 (m, 26H, CONHC $H_2(CH_2)_5$, NCH_2CH_2N, NCH_2CO), 7.10 (s, 1H, NH). ^{13}C NMR ($CDCl_3$, δ, ppm): 25.9, 27.3, 28.7, 29.1, 30.3, 38.5, 51.8, 55.6, 81.8, 172.8, 175.0. MS (ESI$^+$/TOF, *m*/*z*): 693.5 ([M + Na]$^+$, calcd 693.5).

General Procedure for DOTA Conjugation to the Star Copolymers (s(1–4)(e/d)-DOTA). The star copolymer (**s3-e**; 50.8 mg) was dissolved in anhydrous DMF (0.200 mL), followed by the addition of a solution of tris(*t*-butyl) protected DOTA amine (**3**, 13.7 mg) in anhydrous DMF (0.200 mL). The mixture was then heated at 50 °C for 30 h. The solution was poured into diethyl ether to precipitate the polymer. Unreacted **3** was removed by exhaustive centrifugation in a centricon tube (YM-30) with DMF, followed by reprecipitation into diethyl either. The precipitate was collected and dried in vacuo, resulting in a white powder (yield: 35.3 mg, 58%). M_n (DMF): 227 kDa, PDI: 1.24. ^{1}H NMR ($CDCl_3$, δ, ppm): 1.05–2.00 (m, CH, CH_2), 1.35–1.50 (s, *t*Bu), 2.70–3.30 (br m, $CNCH_3$, succinimide CH_2), 3.39 (s, OCH3), 3.50–3.85 (s, OCH_2CH_2O).

General Procedure for Deprotection of *tert*-butyl Group in the Star Copolymers. Each copolymer (ca. 30 mg) was dissolved in dichloromethane (5.0 mL), and trifluoroacetic acid (TFA, 1.0 mL) was added. The solution was stirred overnight at room temperature and concentrated in vacuo. The residue was dissolved in dichloromethane, triturated with hexanes, and excess solvent was removed in vacuo; the cycle was repeated twice to remove residual TFA. The oily residue was then dissolved in DMSO (15 mL) at 60–70 °C, and deionized water (15 mL) was added and stirred for 2 h at the same temperature. The polymeric particles were purified by centrifugation with Centricon tubes (YM-100) in Milli-Q water to eliminate DMSO. After extensive washing, the polymeric particles were then reconstituted in Milli-Q water (3 mg/mL) and stored in a refrigerator at 4 °C for further use.

^{64}Cu-Radiolabeling of DOTA-Conjugated Arm or Star Copolymers. ^{64}Cu-chloride in 0.5 M $HCl_{(aq)}$ was converted to ^{64}Cu-acetate by addition of an appropriate volume of 0.1 M ammonium acetate buffer (pH 7.0) to the solution. An aqueous solution of the polymeric particle with deprotected-DOTA (3 mg/mL) was 2-fold diluted with acetate buffer and added to the solution of ^{64}Cu-acetate (2–5 mCi). After 1 h incubation at 80 °C, 10 mM diethylenetriaminepentaacetic acid (DTPA, 5.0 μL) was added and the labeling mixture was incubated for 10 min at room temperature. Zeba desalt spin columns were used to separate the radiolabeled product from residual free ^{64}Cu and/or complex of ^{64}Cu/DTPA. The labeling yield was determined by radio-ITLC analysis (^{64}Cu-DOTA-copolymers: R_f = 0.0, ^{64}Cu-acetate/^{64}Cu -DTPA: R_f = 0.9). After DTPA challenge and Zeba purification, the RCP of the samples was determined by radio-FPLC. Samples with RCP > 95% were used for animal studies.

The product was then diluted with 10 mM PBS (pH 7.4) to prepare appropriate doses for biodistribution and imaging studies. The in vitro stability (in mouse serum and PBS) of the ^{64}Cu-labeled polymeric particles was evaluated by radio-ITLC analysis at different time points up to 48 h.

The amount of DOTA groups conjugated to the each polymeric species was determined by adding each copolymer (100 μg) with a known amount of "hot plus cold" Cu-acetate (a nonradioactive Cu-acetate solution spiked with 50–100 μCi ^{64}Cu) in ammonium acetate buffer. After 2 h incubation at 80 °C and DTPA challenge, the number of DOTA chelates attached to the nanoparticles was determined from counts per minute (cpm) on the ITLC with the following equation 1:

$$n(\text{chelates}) = \frac{n(\text{copper}) \times \text{cpm}(R_f < 0.3)}{\text{cpm(total)}} \quad (1)$$

where n(chelates) is the number of chelates in the polymer sample, n(copper) is the number of copper atoms (both hot and cold), and cpm(R_f < 0.3) is counts per minute of copper in the lower spot.

Biodistribution Studies. All animal studies were performed in compliance with guidelines set by the Washington University Animal Studies Committee. Normal female Sprague–Dawley rats (180–200 g, n = 4 per time point) were anesthetized with 1–2% vaporized isoflurane and injected with ca. 30 μCi/200 μL of activity via the tail vein (ca. 80–100 μg/kg rat body weight). The rats were anesthetized prior to sacrifice at each time point. Organs and tissues of interest were removed, blotted dry, and weighed. The sample radioactivity was measured in a γ-counter. The total activity in blood was calculated assuming 6% of the rat body weight. Diluted standard doses (1:100) were prepared and counted along with the samples. All the data were corrected for ^{64}Cu decay. The percent injected dose per gram tissue (%ID/g) and the percent injected dose per organ (%ID/organ) values were calculated using the following eqs 2 and 3:

$$\%\text{ID/g} = \frac{(\text{cpm in sample} - \text{background}) \times 10^2}{(\text{decay correction factor}) \times (\text{sample weight}) \times (\text{cpm in standard})} \quad (2)$$

$$\%\text{ID/organ} = \frac{(\text{cpm in sample} - \text{background}) \times 10^2}{(\text{decay correction factor}) \times (\text{cpm in standard})} \quad (3)$$

Small Animal PET Imaging Studies. The imaging studies were carried out using scanners of a MicroPET Focus (CTI-Concorde Microsystems Co.) and a MicroCAT II scanner (CTI-Imtek Co.). Normal Balb/c mice (20–30 g) were anesthetized with 1–2% vaporized isoflurane and injected with ca. 100–200 μCi of ^{64}Cu-labeled particles (1.5–2 mg/kg mouse body weight) in 150 μL of saline via the tail vein. The imaging sessions were performed at 1, 4, and 24 h postinjection (p.i.). MicroPET and microCT image coregistration was accomplished using a landmark registration technique (by using fiducial markers directly attached to the animal bed) and AMIRA image display software (AMIRA, TGS Inc.). Data analysis of microPET images was performed using the manufacturer software (ASIPRO, CTI-Concorde MicroSystem Co.). Data were calculated in terms of the standardized uptake value (SUV) in 3D regions of interests (ROIs) using the following equation 4:

$$\text{SUV} = \frac{\text{radioactivityconcentration in ROI [}\mu\text{Ci/cc]}}{\text{injected dose [}\mu\text{Ci]/animal weight [g]}} \quad (4)$$

One-way analysis of variance (ANOVA) and post hoc multiple comparison (Bonferroni's t test) on the biodistribution data (%ID/g)

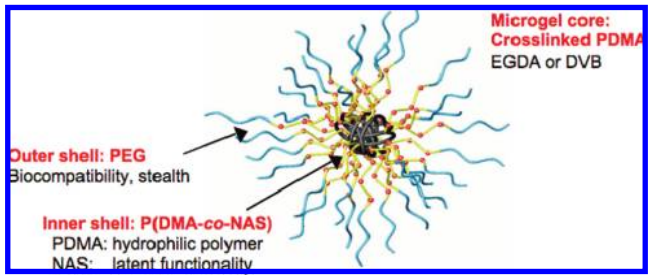

Figure 1. Depiction of PEGylated star copolymer; particles have three layers: (i) outer layer of PEG for stealth, (ii) inner corona of hydrophilic P(DMA-*co*-NAS), and (iii) microgel core.

were performed using Prism v. 4.00 (Graphpad Co.). Groups with $P < 0.01$ were considered significantly different.

Results and Discussion

Synthesis of PEGylated Arm and Star Copolymers. The modular design of core–shell PEGylated star copolymers involves the initial synthesis of functionalized diblock copolymers containing a dormant propagating chain end followed by cross-linking using a difunctional cross-linker, divinyl benzene (DVB), or ethylene glycol diacrylate (EGDA). As the outer block is designed to be PEG, the synthesis begins with the functionalization of PEG with a living free radical initiator and then growth of a diblock copolymer from this macroinitiator. The second block was chosen to be based on *N*,*N*-dimethylacrylamide, due to its water solubility, and *N*-acryloxysuccinimide (NAS), selected as the reactive inner functionality to enable the covalent attachment of a defined number of tris(*t*-butyl) protected DOTA amine (TB-DOTA, **3**) groups in a postmodification step. The star copolymers, therefore, have three distinctive segments (Figure 1): (i) PEG chains forming the outer corona to impart water solubility as well as biological stealth characteristics, (ii) DOTA ligands within the inner shell of PDMA chains for radiolabeling, and (iii) a microgel core covalently linking the star-like structure. It is important to note that, due to the use of the DOTA metal chelator in this system, all synthetic methodology was designed to be metal-free to avoid trace contamination, hence the use of NMP and active-ester amidation chemistries as synthetic strategies. The use of the controlled free radical polymerization technique was also important for fine control over nanoparticle size that is desired for medical applications.

Commercially available monomethoxy PEGs (MW of PEG: 2 or 5 kDa) were coupled to a chloro-functional NMP initiator to obtain macroinitiators, *x*kPEG ($x = 2$ or 5). As shown in Scheme 1, a series of PEG-*b*-P(DMA-*co*-NAS) (**a1**−**a4**) copolymers were synthesized from these macroinitiators with acrylic monomers (hydrophilic DMA and NAS for active ester functionality). The addition of 5 mol % of free nitroxide allowed for controlled polymerization of the acrylic monomers, permitting the molecular weight of the vinyl block to be well-defined.[52,53] The total molecular weights of the arm copolymers were tuned by lengthening the P(DMA-*co*-NAS) blocks; this approach allowed the synthesis of nanostructures with various outer- and inner-shell thicknesses. For example, **a1** and **a2** were synthesized from the 2.0 kDa PEG macroinitiator with shorter and longer PDMA blocks, while **a3** and **a4** were prepared from the corresponding 5.0 kDa derivative with shorter and longer PDMA blocks, as summarized in Table 1. These linear copolymers were then utilized to synthesize PEGylated star copolymers, with the sizes of the star copolymers, and the numbers of active ester sites per polymer chain tuned specifically.

The ability to preform the functionalized diblock copolymers is a key advantage of this strategy and also enhances significantly the ability to characterize both the diblock and subsequent star copolymers fully. The characteristic signals of the DMA and NAS repeat units in the ^{1}H NMR spectra overlap in the range of 2.60–3.20 ppm, which complicated the determination of the relative amount of NAS (Scheme 2). To determine the relative amount of active ester, the block copolymer was allowed to undergo reaction with a large excess of isoamylamine (to ensure complete functionalization) and the dimethyl group at 0.87–0.90 ppm, assignable to the isoamylamine moiety, was used to estimate the quantity of NAS in the parent copolymer (Figure 2). The extent of incorporation of each component of the arm copolymer (DP of PEG/PDMA/PNAS) was then determined (Table 1). Gel permeation chromatography (GPC) traces of the arm copolymers showed monomodal peaks with narrow distributions, implying that well-controlled diblock copolymers were synthesized (Figure 3). On the basis of calculations from the ^{1}H NMR spectroscopy data, the total M_n of each arm copolymer and weight percentage of PEG segments were determined, as given in Table 1. These MWs were in good agreement with the M_ns obtained from MALS measurements (Table 2).

Building on the pioneering work of Qiao and Matyjaszewski,[35–37] the star-shaped copolymers were prepared using NMP from PEGylated arm block copolymers (**a1**−**a4**), a cross-linker (DVB or EGDA), and DMA in DMF at 120 °C (Scheme 3). Each of the 2 kDa/5 kDa PEGylated star copolymers were designed with DVB or EGDA cross-linkers to lead to cores with different levels of reactivity, hydrophobicity, and glass transition temperature. Four different arm copolymers were used to synthesize six star copolymers of various sizes and core functionalities: 2 kDa PEG-*b*-P(DMA-*co*-NAS) stars with EGDA core (**s1-e**), higher molecular weight 2 kDa PEG-*b*-P(DMA-*co*-NAS) stars with DVB core (**s2-d**) or EGDA core (**s2-e**), 5 kDa PEG-*b*-P(DMA-*co*-NAS) stars with DVB core (**s3-d**) or EGDA core (**s3-e**), and higher molecular weight 5 kDa PEG-*b*-P(DMA-*co*-NAS) stars with EGDA core (**s4-e**).

The star formation reaction was optimized as follows: the general feeding ratio of the macroinitiator (MI; i.e., arm copolymers, **a1**−**a4**) and each monomer was determined to be [MI/DMA/X-linker = 1/10/10 (molar equiv)] for **s1-e**, **s2-d**, **s3-d**, and **s3-e**. The reaction of the longer arm copolymers with less reactive EGDA was conducted with slightly higher loading of EGDA ([MI/DMA/EGDA = 1/10/12 (molar equiv.)] for **s2-e** and [= 1/10/15 (molar equiv)] for **s4-e**). The reaction time was also critical to minimize the amount of undesirable high MW impurities, presumably star-star coupled products. The optimal reaction time at 120 °C was determined to be 46–50 h for star copolymers with EGDA cores and to be 22–24 h for stars with DVB cores. Purification of the crude star copolymers was carried out by means of fractional precipitation (Figure 4). The large difference in MW between the arm and star copolymers led to differing solubilities in acetone, thus enabling purification of the star copolymers.

In Table 2, a library of PEG-containing arm and star copolymers synthesized by NMP are described, including GPC (RI in DMF and MALS in chloroform) and DLS (in water) results. Each arm copolymer and corresponding star copolymer show good agreement between the measurements in GPC-RI and GPC-MALS. According to GPC-MALS data, the number of arms per star copolymer is estimated to be 10–22, depending on: (i) the length of arm copolymer, (ii) the amount of the cross-

Scheme 1. Synthesis of PEGylated Arm Copolymer, PEG-*b*-P(DMA-*co*-NAS) in NMRP

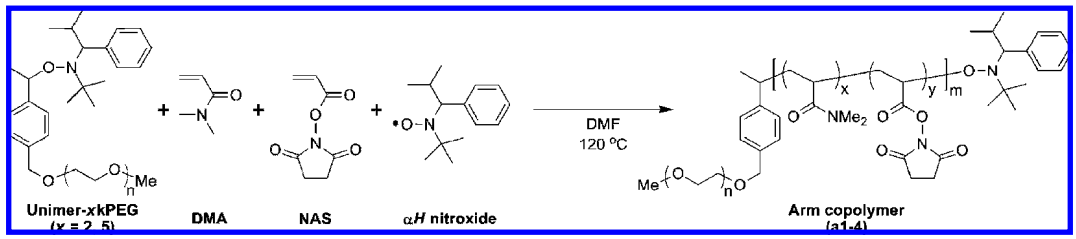

Table 1. PEGylated Arm Copolymers Based on ^{1}H NMR Spectroscopy

arm copolymer	DP[a] PEG	PDMA	PNAS	total MW (kDa)	PEG content (wt %)
a1	45	62	12	10.2	20
a2	45	120	16	16.6	12
a3	114	48	10	11.4	44
a4	114	220	16	29.5	17

[a] Approximate degree of polymerization of each component in the arm copolymer, calculated from ^{1}H NMR integration.

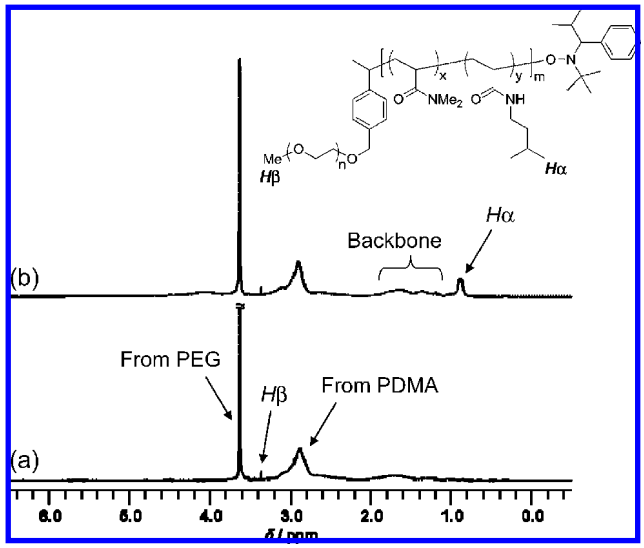

Figure 2. ^{1}H NMR spectra of (a) before and (b) after the amidation reaction with isoamylamine.

linker added, (iii) the reaction time, and (iv) the reactivity of the cross-linkers, in agreement with previous work from Qiao.[35]

Size Distribution of the Polymeric Nanoparticles. The first parameter explored was the size of the star-like copolymer nanoparticles. The sizes of the arm and star copolymers were evaluated in aqueous media by DLS at 25 °C. There was a correlation between D_hs of the star copolymers measured by DLS and M_ns measured by GPC-MALS. From the largest to the smallest, the size distribution of the star copolymers in water was as follows: the high molecular weight 5 kDa PEG star (70.4 ± 8.8 nm, **s4-e**) > the high molecular weight 2 kDa PEG star (67.9 ± 8.0 nm for **s2-e**, 61.4 ± 4.1 nm for **s2-d**) > 2 kDa PEG star (37.3 ± 7.9 nm, **s1-e**) > 5 kDa PEG star (33.7 ± 5.0 nm for **s3-e**, 25.1 ± 2.8 nm **s3-d**). Despite the fact that the molecular weight of **a1** was less than **a3**, **s1-e** was larger than both **s3-d** and **s3-e**. This result is likely due to the higher number of arm copolymers per star-shaped structure for **s1-e** than **s3-d** or **s3-e**, respectively (22.1 arms for **s1-e** compared to 11.1 and 11.9 arms for **s3-d** and **s3-e**, respectively). Comparing DVB and EGDA cores in the similar star copolymers (**s2-d** vs **s2-e**; **s3-d** vs **s3-e**), stars with EGDA cores showed slightly larger D_hs. Thus, the diameters of the star copolymers can be modulated through several modifications, including length of arm copolymer as well as PEG chain length, cross-link density, and microgel core structure.

DOTA Conjugation to Arm and Star Copolymers. Having prepared a range of internally functionalized core–shell star copolymers, the attachment of imaging groups was required. DOTA derivatives have been employed as copper chelators in radiopharmaceuticals[48,58] and to incorporate the DOTA functionality into the proposed nanostructures an amine-functionalized tris(*t*-butyl)-protected DOTA (TB-DOTA, **3**) was synthesized as shown in Scheme 4. Initial amidation of tris(*t*-butyl)-protected DOTA with benzyloxycarbamate-protected diamine was performed, followed by hydrogenation to afford DOTA amine (**3**).[59]

The conjugation of DOTA to the star and arm copolymers was carried out in DMF at 50 °C. The active ester group of NAS, copolymerized with DMA in the second block of the arm copolymers, enabled this postmodification to afford DOTA-conjugated copolymers (**a*n*-DOTA**, n = 2–4; **s*n′x*-DOTA**, $n′$ = 1–4, x = e,d), which were confirmed by ^{1}H NMR spectroscopy. While GPC profiles show little change before and after conjugation (Figure 5), a characteristic *t*-butyl signal assignable to the DOTA molecule appears at 1.49 ppm in the ^{1}H NMR spectrum of the purified DOTA conjugated arm and star copolymers. The tris(*t*-butyl) groups were removed under acidic conditions using 10 vol % TFA in dichloromethane, and subsequent purification was conducted by centrifugal filtration with gradual solution change from DMSO to water.

Isotopic dilution assay (IDA) with a mixture of "hot plus cold" copper (a Cu(II) solution of known concentration, spiked with ^{64}Cu) was run, following the deprotection of the DOTA moieties, to test the conjugation of DOTA to the copolymers

Scheme 2. Amidation Reaction with Isoamylamine and PEG-*b*-P(DMA-*co*-NAS)

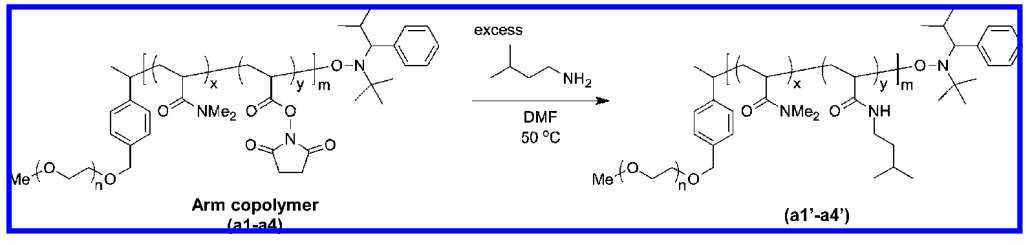

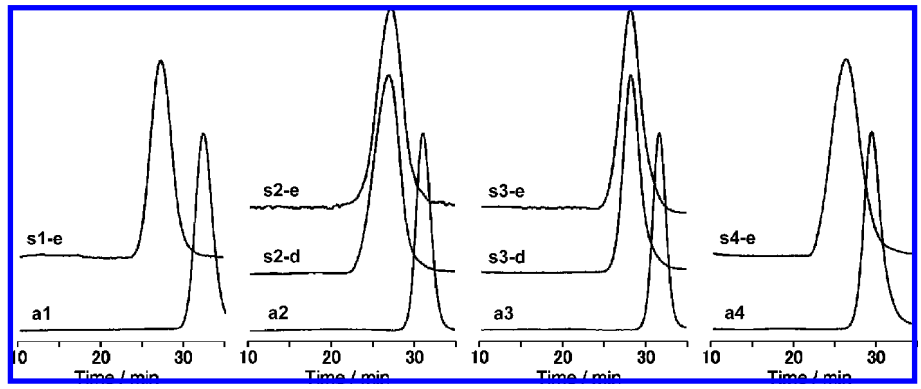

Figure 3. GPC profiles of arm/star copolymers in DMF. Each M_n and PDI are summarized in Table 2.

Table 2. Star Copolymers and the Corresponding Arm Copolymers.

		GPC-RI-DMF[a]		GPC-MALS-CF[b]			DLS
arm or star copolymer		M_n (*k*Da)	PDI	M_n (*k*Da)	PDI	N_{arm}[c] (star)	D_h[d] (nm)
a1	Arm	35.7	1.17	12.4	1.03		3.6 ± 0.6, 92.1 ± 9.4
s1-e	Star/EGDA	271	1.19	274	1.28	22.1	37.3 ± 7.9
a2	Arm	59.0	1.16	20.6	1.06		3.9 ± 0.6, 190.5 ± 26.1
s2-d	Star/DVB	299	1.22	326	1.29	15.8	61.4 ± 4.1
s2-e	Star/EGDA	290	1.23	287	1.37	13.9	67.9 ± 8.0
a3	Arm	56.3	1.12	16.9	1.09		4.6 ± 0.3, 173.5 ± 6.9
s3-d	Star/DVB	178	1.19	188	1.14	11.1	25.1 ± 2.8
s3-e	Star/EGDA	192	1.22	201	1.15	11.9	33.7 ± 5.0
a4	Arm	132	1.13	43.8	1.11		12.5 ± 0.7, 221.0 ± 11.2
s4-e	Star/EGDA	304	1.25	456	1.24	10.4	70.4 ± 8.8

[a] M_ns and PDIs were determined by standard polystyrene calibration in DMF. [b] M_ns and PDIs were determined by MALS in chloroform. [c] Number of arms per star copolymer was determined by the corresponding M_ns of star and arm copolymers obtained from GPC-MALS-CF. [d] Hydrodynamic diameter and size distribution of the polymeric materials in water at 25 °C were determined by DLS in CONTIN analysis.

Scheme 3. Star Formation from Macroinitiator (Arm Copolymer) and Difunctional Cross-linker by NMP

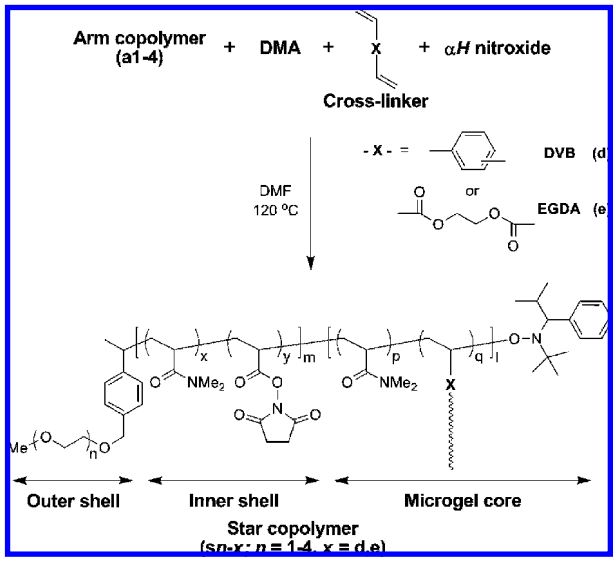

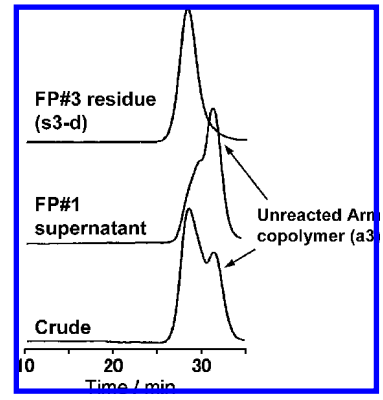

Figure 4. GPC profiles of arm/star copolymers in DMF along with the purification process of fractional precipitation.

as well as their availability to bind copper ions in aqueous solution. Initial experiments, in which the DOTA residues were placed in the hydrophobic core, led to essentially no Cu incorporation, demonstrating the necessity for an aqueous nanoenvironment for the DOTA ligands. As a result, the current design, having a hydrophilic DMA chain to carry the DOTA ligands, incorporated between the PEG shell and the hydrophobic core, was employed and shown to increase, dramatically, the extent of Cu binding. However, the number of DOTA groups detected by IDA was approximately 40–70% lower than that calculated by NMR measurements (Table 3); this partial availability of DOTA functionalities to bind copper is reasonable due to the shielding created by the layer of hydrated PEG chains forming the outer corona in aqueous solution.

Radiolabeling of the Arm/Star Copolymers. The medium-lived positron emitter ^{64}Cu ($T_{1/2}$ = 12.7 h) was chosen in order to track the behavior of the copolymers in vivo for an extended period of time (up to 48 h post injection). Successful labeling (specific activity: 5–10 mCi/mg polymer) was obtained by incubating the DOTA-functionalized copolymers with ^{64}Cu acetate.[33,49,60,61] After 1 h incubation at 80 °C, the loosely bound ^{64}Cu was challenged by the addition of excess diethylenetriaminepentaacetic acid (DTPA), a linear small molecule chelating agent, followed by purification. The radiochemical purity of the purified ^{64}Cu-labeled copolymers was greater than 95%, as determined by radiochemical-fast protein liquid chromatograpy (radio-FPLC) analysis, indicating that greater than 95% of the radioactive ^{64}Cu was retained within the nanosized DOTA-conjugate after 48 h incubation in rat serum at 36 °C in vitro,

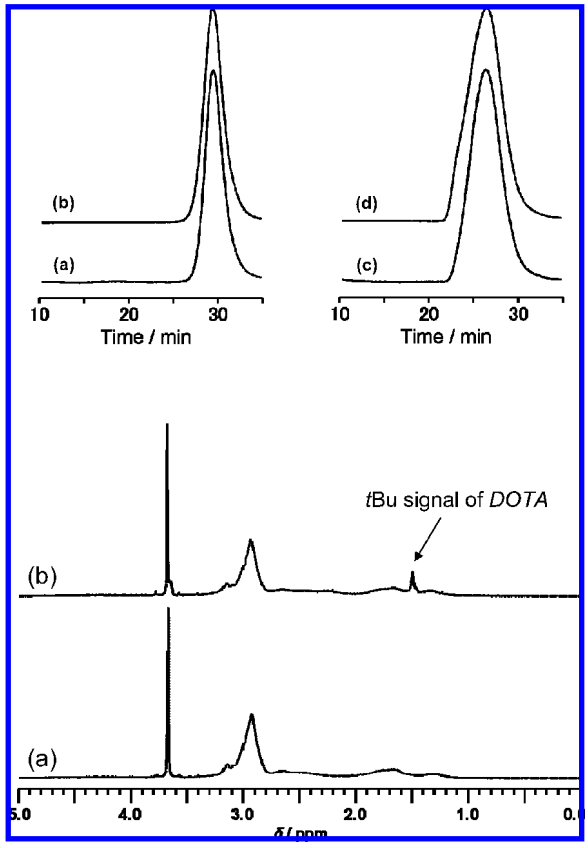

Figure 5. Upper: GPC profiles of arm copolymer **a4** (a) and star copolymer **s4-e** (c) before DOTA conjugation reaction, and after the reaction of the corresponding arm copolymer **a4-DOTA** (b) and star copolymer **s4e-DOTA** (d). Lower: ^{1}H NMR specta of (a) before DOTA conjugation reaction with **s4-e** and (b) after the reaction **s4e-DOTA**.

demonstrating that the radionuclide was stably bound to the DOTA chelators within the star copolymer. The ability to prepare a library of core–shell star polymers with ^{64}Cu specifically located within the interior of the nanostructure allowed the effects of nanoparticle size, shell thickness, etc. on biodistribution to be studied in detail.

Biodistribution Studies. Fast elimination of systemically administered nanoparticles from the circulation is a major drawback for the translation of nanotechnologies to the clinic, especially in the field of sustained drug delivery. The clearance from blood is mainly due to particle sequestration by the MPS with consequent high hepatic and splenic accumulation and, possibly, toxic side effects to these organs.[1,3,5,11,15] Therefore,

Table 3. DOTA Conjugation and the Subsequent Radiolabeling of ^{64}Cu to the Arm and Star Copolymers

	^{1}H NMR	IDA	
arm or star copolymer	N_{DOTA}-NMR[a] (particle)	[DOTA] (/100 μg)	N_{DOTA}-IDA[b] (particle)
a2	2.8	6.1×10^{-9}	1.3 (4)[c]
a3	1.8	4.0×10^{-9}	0.7
a4	4.6	4.8×10^{-9}	2.1
s1e	44.2	1.0×10^{-8}	27.4
s2d	46.3	1.1×10^{-8}	36
s2e	44.5	6.6×10^{-9}	19 (24)[c]
s3d	24.9	5.3×10^{-9}	10
s3e	27.4	6.3×10^{-9}	13
s4e	49.1	6.8×10^{-9}	31

[a] Estimated by multiplying the number of DOTA calculated from ^{1}H NMR spectrum and N_{arm} obtained from Table 2. [b] Estimated from [DOTA] and the M_n of GPC-MALS-CF obtained from Table 2. [c] Data in brackets were obtained shortly after arm/star were dissolved in solution.

to evaluate the influence of PEG length, particle size, and core composition on the stealth characteristics of our new nanomaterials in vivo, we focused our interest on blood retention, accumulation in the major MPS organs (liver and spleen), hepatobiliary, and renal excretion following the intravenous injection of ^{64}Cu-labeled star copolymers in normal Sprague–Dawley rats ($n = 4$ per time point). The data for these organs as a function of sample are shown in Figure 6 and Table 4, and groups with $P < 0.05$ (one-way analysis of variance and post hoc multiple comparison (Bonferroni's t test)) were considered to be significantly different.

As expected, the linear arm copolymers (**a2** and **a3**) with molecular weights less than 20 kDa disappeared rapidly from the bloodstream (Figure 6A,B) and did not accumulate in liver (parts C and D of Figure 6, respectively) or spleen (parts E and F of Figure 6, respectively). This result is due to the fact that the molecular weights of these linear polymers are below the renal threshold for glomerular filtration[62] and, therefore, undergo rapid urinary excretion (Table 4). When considering the star copolymers obtained from the 2 and 5 kDa PEG arms, the influence of the PEG length on the blood retention and MPS uptake is striking. Both series of PEGylated nanosystems were present in high levels in the blood throughout the first hour after intravenous injection. However, at later time points, clearance of the 2 kDa PEG star copolymers from the blood was faster than that of the 5 kDa PEG analogs (parts A and B of Figure 6, respectively). At 48 h post injection, significant amounts of 5 kDa PEG nanoparticles were still circulating in the blood stream, while the 2 kDa PEG stars had cleared. When compared to the linear copolymers, the cross-linked star copolymers were

Scheme 4. Synthesis of Tris(*t*-butyl) Protected DOTA Amine (**3**)[a]

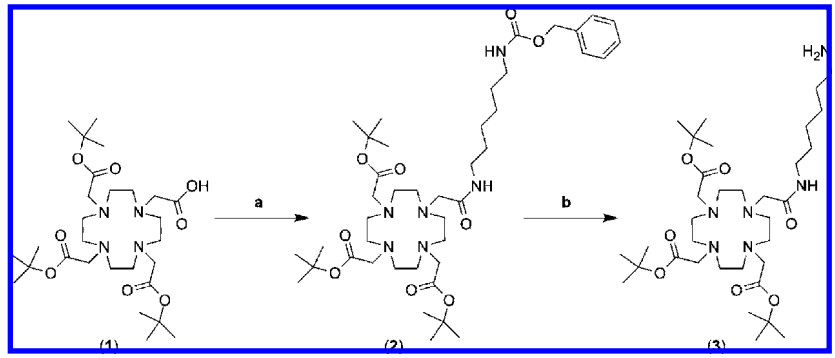

[a] Reaction conditions: (a) *N*-Cbz-1,6-hexanediamine hydrochloride, NHS, HBTU, TEA, in DMF at room temperature for 16 h; (b) Pd/C, H2, in methanol/THF at room temperature for 30 h.

Table 4. Excretion of ^{64}Cu-labeled Arm and Star Copolymers at 48 h Post Injection

	urine[a]	feces[a]
a2	44.2 ± 9.1	11.6 ± 2.2
a3	53.0 ± 9.3	11.7 ± 1.8
s1-e	3.6 ± 0.1	8.2 ± 1.7
s2-e	2.1 ± 0.2	10.4 ± 6.2
s2-d	5.2 ± 1.0	6.4 ± 1.2
s3-e	5.6 ± 0.3	8.2 ± 1.7
s3-d	7.6 ± 0.9	7.5 ± 1.0
s4-d	6.4 ± 0.7	7.3 ± 1.2

[a] Data obtained in normal Sprague–Dawley rats and presented as percent injected dose (%ID) ± standard deviation ($n = 4$, ANOVA: $P < 0.0001$).

eliminated through the sinusoid capillaries of liver and spleen rather than the kidney glomerulus, and the stars exhibited a slower rate of blood clearance.

Noticeably, the length of the PEG chain used to build the arm influenced the blood retention time more than did the nanoparticle size or core composition (Figure 6). In fact, when considering particles with 5 kDa vs 2 kDa PEG chains, the amounts of **s4-e** and **s3-e** circulating in blood were higher than those of **s2-e** and **s1-e**, respectively, up to 24 h post injection, despite the similar sizes and core compositions. Conversely, when comparing the blood clearance of particles with the same PEG chain length, no significant differences were observed between **s2-e** and **s2-d** after the first four hours, or between **s3-e** and **s3-d** at each considered time point, despite the different cores. Similarly, no significant differences were observed between **s1-e** and **s2-e** after the first hour, or between **s3-e** and **s4-e** after 4 h post injection, despite the difference in sizes. Similar considerations apply to the PEG% content in the nanostructures, which is another parameter that can influence the in vivo behavior of the nanoparticles.[8] In fact, despite similar PEG% content, the 5 kDa PEG-containing structures, **s4-e**, circulated longer than did the 2 kDa PEG-containing materials, **s1-e**, up to 24 h post injection, with a similar clearance thereafter.

Eventually, all the intravenously injected particles were eliminated from the blood, even the long circulating ones.[3] In the liver, endothelial cells on the sinusoids, hepatocytes, Kupffer cells, and hepatic stellate cells display phagocytic behavior toward foreign particles and senescent cells.[63] In addition,

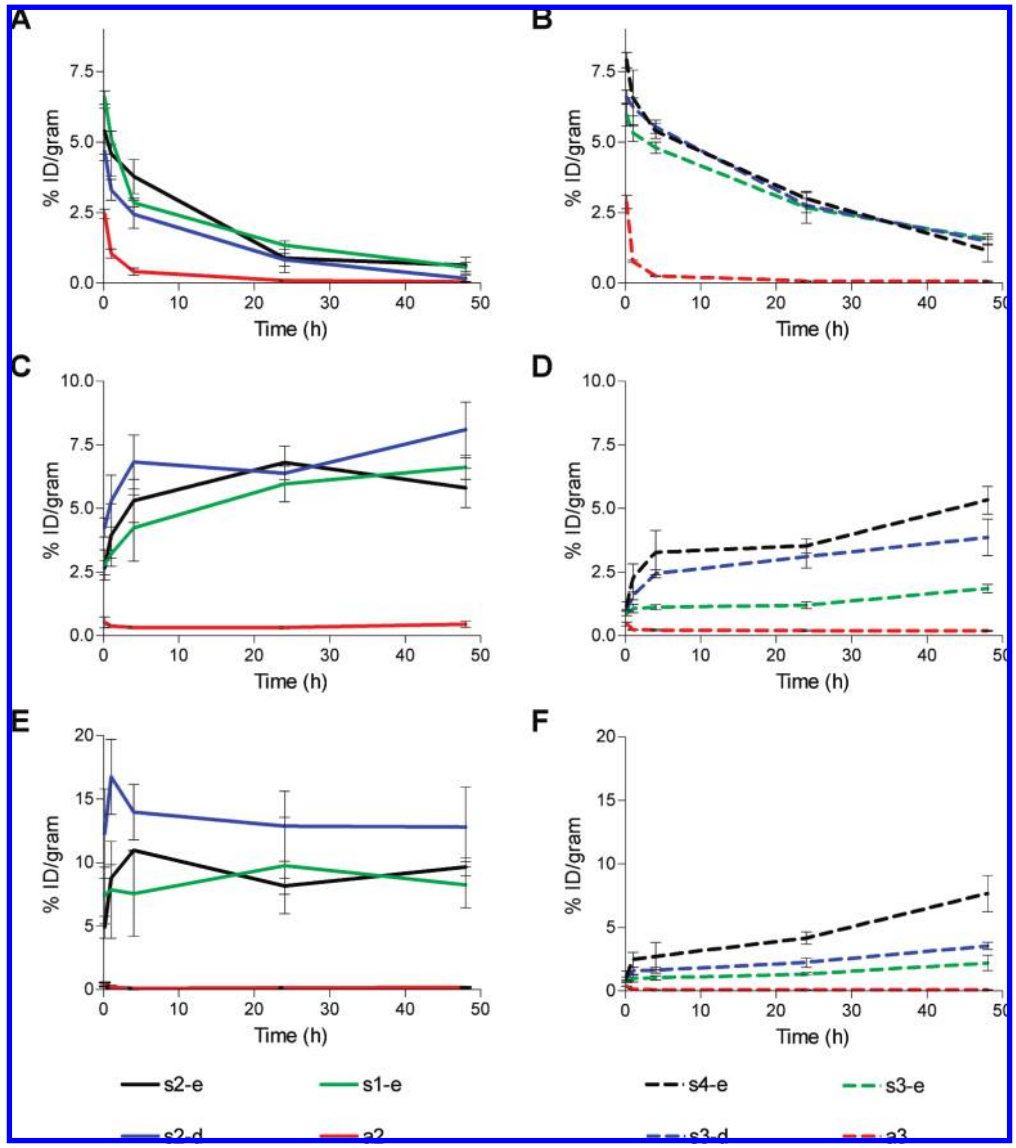

Figure 6. Biodistribution of ^{64}Cu-labeled arm and star copolymers in blood (A,B), liver (C,D), and spleen (E,F) of normal Sprague–Dawley rats (ca. 1.5 MBq/rat, ca. 80 μg/kg rat body weight). Data expressed as percent injected dose per gram tissue (%ID/g). Error bars represent standard deviation ($n = 4$, ANOVA: $P < 0.0001$).

macrophages located in the marginal zone and in the red pulp of the spleen are involved in the clearance of blood borne particles.[64]

The data showed a correlation between the length of the PEG blocks and the hepatic and splenic uptake of the star copolymers. The hepatic accumulation of the 5 kDa PEG **s3-e** was lower than that of the 2 kDa PEG **s1-e** at each considered time point (parts C and D of Figure 6, respectively) regardless of size and core composition. Also, **s4-e** was taken up significantly less than was **s2-e** in the first 24 h after administration and reached comparable levels at later time points. Similar trends were observed in the spleen (parts E and F of Figure 6). Overall, these findings are noteworthy, as blood circulation and MPS uptake of intravenously injected particles are inversely correlated (i.e., the lower the MPS uptake, the longer the blood half-life).

Interestingly, copolymer size and core flexibility affected the hepatic and splenic uptake more than the blood retention, especially for the 5 kDa PEG-containing stars. In fact, **s3-e** accumulated significantly slower than **s4-e** (size effect) and **s3-d** (core effect) in both liver and spleen (parts D and F of Figure 6, respectively). In the 2 kDa PEG star series, the trend is less evident, possibly because of the higher variability within each experimental group. However, the biodistribution data showed a significantly slower splenic uptake of the 2 kDa PEG star copolymer with an EGDA core (**s2-e**) compared to the counterpart containing DVB (**s2-d**) within the first hour post injection, as well as a faster hepatic clearance at later time points. Again, the presence of a similar PEG% content in particles with 5 kDa and 2 kDa PEG chains did not grant comparable behaviors in the MPS. In fact, **s1-e** was taken up by the spleen significantly faster than was **s4-e** within the first hour. On the contrary, no significant difference in liver uptake was found, reasonably due to the fast hepatic accumulation of **s4-e**.

Small Animal Imaging Studies. The high degree of bioavailability and low MPS uptake for the 5 kDa PEG-based star copolymers allows these materials to be used in a clinical environment for imaging of the circulatory system. As a result, normal Balb/C mice ($n = 2$) were administered both the precursor ^{64}Cu-labeled arm copolymers as well as the corresponding star nanostructures and imaged by microPET Focus (Siemens Medical Solutions) at select time points, post injection. Anatomical information on tracer distribution was obtained by attaching fiducial markers directly to the animal bed and by superimposing microPET to microCT images (microCAT II, CTI-Imtek) using a landmark coregistration technique. Examples of small animal PET projection images obtained after the administration of the core–shell star copolymers (**s4-e** and **s2-e**) and a linear arm copolymer (**a3**) are shown in Figure 8. The standardized uptake values (SUVs) calculated in 3D regions of interest (ROIs) drawn on select organs of these mice are shown in Table 5, and additional SUV data are included in the Supporting Information (Table S1). Quantitative analysis of the PET images confirms the long blood retention of the 5 kDa PEG- and 2 kDa PEG-containing nanostructures. In fact, the heart and the major blood vessels (aorta, carotid arteries, and vessels in the orbital area) of the mice injected with **s4-e** and **s2-e** are clearly visible at each time point. Furthermore, the heart SUV of the mice injected with **s2-e** decreased faster than that of the mice injected with **s4-e**, confirming the faster blood clearance of the 2 kDa PEG star copolymer compared to that of the 5 kDa PEG analog. The accumulation of cross-linked star copolymers in MPS organs was also confirmed. The liver was the most noticeable organ in these mice, especially at 4 and 24 h after the administration of **s2-e**, while both copolymers

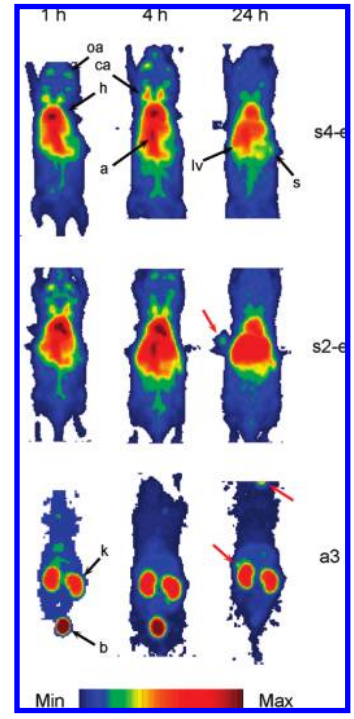

Figure 7. Small animal PET projection images (decay corrected and scaled by min max frame) obtained 1, 4, and 24 h after the administration of select ^{64}Cu-labeled star and arm copolymers in Balb/C mice (ca. 1.5–2 mg/kg mouse body weight; ca. 3.7 MBq/mouse). oa = orbital area; ca = carotid artery; h = heart; lv = liver; a = aorta; s = spleen; k = kidney; b = bladder. Red arrows indicate the fiducial markers used for PET/CT coregistration.

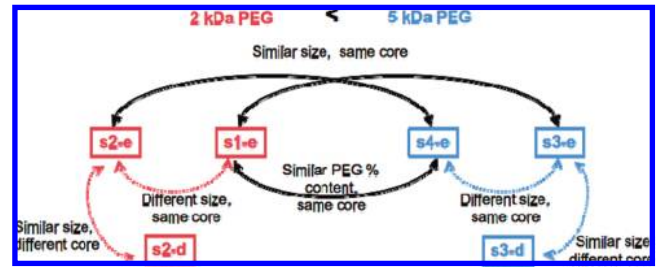

Figure 8. Comparisons of star copolymer biodistributions. Starts made from 5 and 2 kDa PEG arms are separated by color. Comparisons within a given initiator PEG length (colored, dashed lines) show similar/no change in biodistribution behavior. Comparisons between stats of differing the PEG initiator lengths (black, solid arrows) showed varying biodistributions with the 5k stars showing longer blood circulation times in every case.

exhibited little urinary excretion. On the contrary, liver, heart, and blood vessels did not accumulate a significant amount of radioactivity in the mice administered the linear arm (Figure 7, bottom). In these mice, instead, kidney and bladder were the only visible organs due to fast urinary excretion.

Conclusions

A synthetic procedure for the preparation of functionalized, core–shell star copolymers based on nitroxide mediated living radical polymerization has been developed. By coupling of well-defined block copolymer arms through a core cross-linking strategy, a library of linear arm copolymers containing PEG chains of different lengths and reactive chemical functionalities were prepared and converted into their corresponding star copolymers with defined size and core–shell

Table 5. Standardized Uptake Values for Select ^{64}Cu-Labeled Arm and Star Copolymers

	s4-e	s2-e	a3
heart[a]			
1 h	5.22 ± 1.49	4.60 ± 1.42	0.81 ± 0.33
4 h	4.72 ± 0.98	3.24 ± 0.75	0.34 ± 0.10
24 h	3.35 ± 0.17	1.80 ± 0.57	0.11 ± 0.01
liver[a]			
1 h	3.25 ± 1.15	3.28 ± 0.79	0.80 ± 0.23
4 h	2.55 ± 0.87	4.19 ± 0.68	0.59 ± 0.09
24 h	3.24 ± 0.16	4.46 ± 1.17	0.44 ± 0.04
kidney[a]			
1 h	2.28 ± 0.55	2.04 ± 0.49	2.66 ± 0.31
4 h	2.05 ± 0.47	1.90 ± 0.36	2.67 ± 0.38
24 h	1.92 ± 0.13	1.79 ± 0.10	1.83 ± 0.16

[a] Data calculated in 3D regions of interest drawn on select organs of Balb/C mice ($n = 2$) and corrected for ^{64}Cu radioactive decay.

morphology. The specific placement of DOTA ligands in an internal, hydrophilic environment allowed efficient ^{64}Cu-labeling and use of these materials as nanoscopic imaging agents. The biodistribution evaluation in normal rodents has shown a distinct correlation between the length of the PEG grafts and the in vivo behavior of these nanostructures. In fact, the use of arm copolymers containing 5 kDa PEG chains increased the blood retention and lowered the burden in MPS organs, such as liver and spleen, compared to 2 kDa PEG. Not only is a significant improvement for these nanostructured materials observed over conventional small molecule agents as imaging tracers, the dramatic effects of PEG length on the blood retention time and uptake in MPS organs clearly show the benefit of a modular, synthetic approach. Nanomaterials such as these could enhance targeted imaging of disease states and enable novel therapies for lung and cardiovascular injuries.

Acknowledgment. We thank Nicole Fettig, Margaret Morris, Dawn Werner, Lori Strong, Ann Stroncek, and Jerrel Rutlin for technical assistance in the biodistribution and imaging studies. This material is based upon work supported by the National Heart Lung and Blood Institute of the National Institutes of Health, as a Program of Excellence in Nanotechnology (HL080729). The production of ^{64}Cu is supported by a grant from the National Cancer Institute (CA86307) and the characterization of the polymeric materials was enabled by the use of facilities supported by the MRSEC Program of the National Science Foundation (DMR-0520415).

References and Notes

(1) Moghimi, S. M. *Anticancer Agents Med. Chem.* **2006**, *6* (6), 553–561.
(2) Torchilin, V. P. *Adv. Drug Delivery Rev.* **2006**, *58* (14), 1532–1555.
(3) Moghimi, S. M.; Hunter, A. C.; Murray, J. C. *Pharmacol. Rev.* **2001**, *53* (2), 283–318.
(4) Brigger, I.; Morizet, J.; Aubert, G.; Chacun, H.; Terrier-Lacombe, M.-J.; Couvreur, P.; Vassal, G. *J. Pharmacol. Exp. Ther.* **2002**, *303* (3), 928–936.
(5) Drummond, D. C.; Meyer, O.; Hong, K.; Kirpotin, D. B.; Papahadjopoulos, D. *Pharmacol. Rev.* **1999**, *51* (4), 691–744.
(6) Dunn, S. E.; Brindley, A.; Davis, S. S.; Davies, M. C.; Illum, L. *Pharm. Res.* **1994**, *11* (7), 1016–1022.
(7) Gabizon, A.; Shmeeda, H.; Horowitz, A. T.; Zalipsky, S. *Adv. Drug Delivery Rev.* **2004**, *56* (8), 1177–1192.
(8) Gref, R.; Luck, M.; Quellec, P.; Marchand, M.; Dellacherie, E.; Harnisch, S.; Blunk, T.; Muller, R. H. *Colloids Surf. B* **2000**, *18* (3–4), 301–313.
(9) Kommareddy, S.; Amiji, M. *J. Pharm. Sci.* **2006**, *96* (2), 397–407.
(10) Niidome, T.; Yamagata, M.; Okamoto, Y.; Akiyama, Y.; Takahashi, H.; Kawano, T.; Katayama, Y.; Niidome, Y. *J. Controlled Release* **2006**, *114* (3), 343–347.
(11) Owens, D. E., III; Peppas, N. A. *Int. J. Pharm.* **2006**, *307* (1), 93–102.
(12) Shi, B.; Fang, C.; Pei, Y. *J. Pharm. Sci.* **2006**, *95* (9), 1873–1887.
(13) Kwon, G.; Suwa, S.; Yokoyama, M.; Okano, T.; Sakurai, Y.; Kataoka, K. *J. Controlled Release* **1994**, *29* (1–2), 17–23.
(14) Otsuka, H.; Nagasaki, Y.; Kataoka, K. *Curr. Opin. Colloid Interface Sci.* **2001**, *6* (1), 3–10.
(15) Moghimi, S. M.; Szebeni, J. *Prog. Lipid Res.* **2003**, *42* (6), 463–478.
(16) Mosqueira, V. C. F.; Legrand, P.; Gulik, A.; Bourdon, O.; Gref, R.; Labarre, D.; Barratt, G. *Biomaterials* **2001**, *22* (22), 2967–2979.
(17) Stolnik, S.; Daudali, B.; Arien, A.; Whetstone, J.; Heald, C. R.; Garnett, M. C.; Davis, S. S.; Illum, L. *Biochim. Biophys. Acta* **2001**, *1514* (2), 261–279.
(18) Adams, M. L.; Lavasanifar, A.; Kwon, G. S. *J. Pharm. Sci.* **2003**, *92* (7), 1343–1355.
(19) Bae, Y.; Fukushima, S.; Harada, A.; Kataoka, K. *Angew. Chem., Int. Ed.* **2003**, *42* (38), 4640–4643.
(20) Kakizawa, Y.; Harada, A.; Kataoka, K. *Biomacromolecules* **2001**, *2* (2), 491–497.
(21) Kim, S. Y.; Shin, I. L. G.; Lee, Y. M.; Cho, C. S.; Sung, Y. K. *J. Controlled Release* **1998**, *51* (1), 13–22.
(22) Kwon, G.; Naito, M.; Yokoyama, M.; Okano, T.; Sakurai, Y.; Kataoka, K. *Langmuir* **1993**, *9* (4), 945–949.
(23) Nasongkla, N.; Bey, E.; Ren, J.; Ai, H.; Khemtong, C.; Guthi, J. S.; Chin, S. F.; Sherry, A. D.; Boothman, D. A.; Gao, J. *Nano Lett.* **2006**, *6* (11), 2427–2430.
(24) Torchilin, V. P. *Pharm. Res.* **2007**, *24* (1), 1–16.
(25) Bronstein, L. M.; Chernyshov, D. M.; Timofeeva, G. I.; Dubrovina, L. V.; Valetsky, P. M.; Khokhlov, A. R. *Langmuir* **1999**, *15* (19), 6195–6200.
(26) Yu, Y.; Zhang, L.; Eisenberg, A. *Macromolecules* **1998**, *31* (4), 1144–1154.
(27) Chen, Y.; Tavakley, A. E.; Mathiason, T. M.; Taton, T. A. *J. Polym. Sci., Part A: Polym. Chem.* **2006**, *44* (8), 2604–2614.
(28) Huang, H.; Hoogenboom, R.; Leenen, M. A. M.; Guillet, P.; Jonas, A. M.; Schubert, U. S.; Gohy, J. F. *J. Am. Chem. Soc.* **2006**, *128* (11), 3784–3788.
(29) Huo, Q.; Liu, J.; Wang, L. Q.; Jiang, Y.; Lambert, T. N.; Fang, E. *J. Am. Chem. Soc.* **2006**, *128* (19), 6447–6453.
(30) Jaturanpinyo, M.; Harada, A.; Yuan, X.; Kataoka, K. *Bioconjugate Chem.* **2004**, *15* (2), 344–348.
(31) Li, Y.; Lokitz, B. S.; Armes, S. P.; McCormick, C. L. *Macromolecules* **2006**, *39* (8), 2726–2728.
(32) Rheingans, O.; Hugenberg, N.; Harris, J. R.; Fischer, K.; Maskos, M. *Macromolecules* **2000**, *33* (13), 4780–4790.
(33) Sun, X.; Rossin, R.; Turner, J. L.; Becker, M. L.; Joralemon, M. J.; Welch, M. J.; Wooley, K. L. *Biomacromolecules* **2005**, *6* (5), 2541–2554.
(34) O'Reilly, R. K.; Joralemon, M. J.; Hawker, C. J.; Wooley, K. L. *J. Polym. Sci., Part A: Polym. Chem.* **2006**, *44*, 5203–5217.
(35) Connal, L. A.; Gurr, P. A.; Qiao, G. G.; Solomon, D. H. *J. Mater. Chem.* **2005**, *15* (12), 1286–1292.
(36) Lapienis, G. *J. Polym. Sci., Part A: Polym. Chem.* **2007**, *45*, 5017–5021.
(37) Xia, J.; Zhang, X.; Matyjaszewski, K. *Macromolecules* **1999**, *32* (13), 4482–4484.
(38) Bosman, A. W.; Heumann, A.; Klaerner, G.; Benoit, D.; Frechet, J. M. J.; Hawker, C. J. *J. Am. Chem. Soc.* **2001**, *123* (26), 6461–6462.
(39) Bosman, A. W.; Vestberg, R.; Heumann, A.; Frechet, J. M. J.; Hawker, C. J. *J. Am. Chem. Soc.* **2003**, *125* (3), 715–728.
(40) Helms, B.; Guillaudeu, S. J.; Xie, Y.; McMurdo, M.; Hawker, C. J.; Fréchet, J. M. J. *Angew. Chem., Int. Ed.* **2005**, *44* (39), 6384–6387.
(41) Giguère, G.; Zhu, X. X. *J. Polym. Sci., Part A: Polym. Chem.* **2007**, *45*, 4173–4178.
(42) Gauthier, M. *J. Polym. Sci., Part A: Polym. Chem.* **2007**, *45*, 3803–3810.
(43) Hirao, A.; Hayashi, M.; Loykulnant, S.; Sugiyama, K.; Ryu, S. W.; Haraguchi, N.; Matsuo, A.; Higashihara, T. *Prog. Polym. Sci.* **2005**, *30* (2), 111–182.
(44) Kanaoka, S.; Fujita, Y.; Higashimura, T. *Macromol. Rapid Commun.* **2000**, *21* (5), 218–222.
(45) Kanaoka, S.; Koyama, C.; Higashimura, T. *Polym. J.* **2003**, *35* (2), 167–172.
(46) Shibata, T.; Kanaoka, S.; Aoshima, S. *J. Am. Chem. Soc.* **2006**, *128* (23), 7497–7504.
(47) Matyjaszewski, M.; Spanskwick, J. *Mater. Today* **2005**, *8* (3), 26–33.
(48) Sun, X.; Anderson, C. J. *Methods Enzymol.* **2004**, *386*, 237–261.

(49) Pressly, E. D.; Rossin, R.; Hagooly, A.; Fukukawa, K. I.; Messmore, B. W.; Welch, M. J.; Wooley, K. L.; Lamm, M. S.; Hule, R. A.; Pochan, D. J.; Hawker, C. J. *Biomacromolecules* **2007**, *8* (10), 3126–3134.
(50) Rossin, R.; Sun, X.; Fang, H.; Turner, J.; Li, X.; Wooley, K. L.; Taylor, J.-S.; Welch, M. J. Small animal PET imaging of MCF-7 tumors in mice with PNA-conjugated nanoparticles targeting the unr mRNA. *J Labelled Compd. Radiopharm.* **2005**, *48* (S1), S35.
(51) Yuan, J. C.; You, Y. Z.; Lu, X.; Muzik, O.; Oupicky, D.; Peng, F. Y. *Mol. Imaging* **2007**, *6* (1), 10–17.
(52) Benoit, D.; Chaplinski, V.; Braslau, R.; Hawker, C. J. *J. Am. Chem. Soc.* **1999**, *121* (16), 3904–3920.
(53) Hawker, C. J.; Bosman, A. W.; Harth, E. *Chem. Rev.* **2001**, *101* (12), 3661–3688.
(54) Pollak, A.; Blumenfeld, H.; Wax, M.; Baughn, R. L.; Whitesides, G. M. *J. Am. Chem. Soc.* **1980**, *102* (20), 6324–6336.
(55) McCarthy, D. W.; Shefer, R. E.; Klinkowstein, R. E.; Bass, L. A.; Margeneau, W. H.; Cutler, C. S.; Anderson, C. J.; Welch, M. J. *Nucl. Med. Biol.* **1997**, *24* (1), 35–43.
(56) Lu, Z. R.; Wang, X. H.; Parker, D. L.; Goodrich, K. C.; Buswell, H. R. *Bioconjugate Chem.* **2003**, *14* (4), 715–719.
(57) Zhang, Z. R.; Liang, K. X.; Bloch, S.; Berezin, M.; Achilefu, S. *Bioconjugate Chem.* **2005**, *16* (5), 1232–1239.
(58) Wadas, T. J.; Wong, E. H.; Weisman, G. R.; Anderson, C. J. *Curr. Pharm. Des.* **2007**, *13* (1), 3–16.
(59) Mattila, K.; Siltainsuu, J.; Balaspiri, L.; Ora, M.; Lonnberg, H. *Org. Biomol. Chem.* **2005**, *3* (16), 3039–3044.
(60) Liu, Z.; Cai, W.; He, L.; Nakayama, N.; Chen, K.; Sun, X.; Chen, X.; Dai, H. *Nat. Nanotechnol.* **2007**, *2* (1), 47–52.
(61) Rossin, R.; Pan, D.; Qi, K.; Turner, J. L.; Sun, X.; Wooley, K. L.; Welch, M. J. *J. Nucl. Med.* **2005**, *46* (7), 1210–1218.
(62) Seymour, L. W.; Duncan, R.; Strohalm, J.; Kopecek, J. *J. Biomed. Mater. Res.* **1987**, *21* (11), 1341–1358.
(63) Popielarski, S. R.; Hu-Lieskovan, S.; French, S. W.; Triche, T. J.; Davis, M. E. *Bioconjugate Chem.* **2005**, *16* (5), 1071–1080.
(64) Moghimi, S. M. *Adv. Drug Delivery Rev.* **1995**, *17* (1), 103–115.

BM7014152